Biophysical Journal Volume 67 July 1994 217–226

Lipid Mono- and Bilayer Supported on Polymer Films: Composite Polymer-Lipid Films on Solid Substrates

Martin Kühner,* Robert Tampé,*‡ and Erich Sackmann*

*Physik Department, Biophysics Group, Technische Universität München, D-85748 Garching/München, and ‡Max-Planck-Institut für Biochemie, D-82152 Martinsried/München, Germany

ABSTRACT We report the deposition of lipid monolayers and bilayers on polyacrylamide films deposited by radical chain reaction onto solid substrates in aqueous solutions. Polymer films of various degrees of monomer density and cross-linking are prepared. Lateral diffusion and fluorescent probe permeation measurements yield insight into the continuity of the lipid layers and show that monolayers exposed to air are much less sensitive towards polymer heterogeneities than bilayers below water, which is explained in terms of the wetting laws. The diffusion studies of lipid and lipopeptide probes yield absolute values of the frictional coefficients between the lipid layer and the polymer films and allow one to estimate the surface viscosity of the polymer film. The potential applications of supported membranes on soft thin polymer films for the preparation of biofunctionalized surfaces or biocompatible receptive surfaces for biosensors are discussed.

INTRODUCTION

Supported lipid layers on solid substrates offer various scientific and practical applications (as biosensors). Deposited on suitably pretreated glass substrates, the membranes can be separated from the solid substrate surface by thin lubricating aqueous layers and thus exhibit the same structural thermodynamic and molecular dynamic properties as free bilayers (Tamm and McConnell, 1985; Merkel et al., 1989). Such planar membranes offer unique advantages for fundamental studies in membrane biophysics because they allow the application of powerful surface sensitive techniques such as FTIR-spectroscopy, ellipsometry, surface plasmon spectroscopy, neutron surface scattering, and fluorescence spectroscopy in the evanescent field. By means of vesicle fusion on glass beads, bilayers with well defined curvature can be prepared that offer unique advantages for NMR-studies of the molecular structure and dynamics (Bayerl and Bloom, 1990). The frictional coupling can lead to the break-down of the membrane two-dimensionality, resulting in a remarkable slowing down of lateral diffusion. This effect can be exploited for measurements of coefficients of friction between the two opposing leaflets of a supported bilayer and of molecular radii of membrane-bound amphiphiles such as macro lipids and proteins (Evans and Sackmann, 1988; Merkel et al., 1989).

The present work was motivated by our attempts to apply supported bilayers as biosensors for electrical (e.g., by impedance spectroscopy) and micro-optical detection (e.g., by surface plasmon spectroscopy) of ligand binding. In previous studies in our group, it was shown that the combination of capacitance measurement and surface plasmon spectroscopy provides a powerful tool for the detection of specific and nonspecific ligand binding and to test the electric tightness of supported bilayers (Stelzle et al., 1993). But it also turns out that additional methods of signal amplification are required, such as the local enrichment of receptors by microelectrophoresis (Stelzle et al., 1992) or ligand-mediated formation of conducting pores. It appears that by separating the bilayers from the solid surface by a soft polymer cushion, the electrophoretic separation and enrichment is more easily achieved (C. Dietrich and R. Tampé, unpublished data). The separation of the bilayer from the solid substrates by the polymer film is also essential for functional reconstitution of membrane proteins including channels, transporters, and pores. Moreover, it is hoped that it allows the incorporation of membrane-spanning receptors into the supported bilayer because the hydrophilic part of the protein on the side facing the substrate can be kept in a pseudo-cellular environment.

One purpose of the present work is to report the preparation of such a novel type of supported membrane-polymer compound films and to show that lateral diffusion measurements of membrane-bound ligands provide a sensitive test for the continuity and fluidity of the supported membranes, but also to allow information on the heterogeneity of the polymer film. A second purpose is to report the measurement of the direct coefficients of friction between the lipid layer and the polymer film and of the surface viscosity of the polymer film. We chose lipopeptides as models because they

Received for publication 27 December 1993 and in final form 4 April 1994.

Address reprint requests to Robert Tampé, Max-Planck-Institut für Biochemie, Molekulare Strukturbiologie, Am Klopferspitz 18a, D-82152 Martinsried, München, Germany. Tel.: 011-49-89-8578-2646; Fax: 011-49-89-8578-2641.

Abbreviations used: PA, polyacrylamide; *T*, weight percentage of monomers (acrylamide and bisacrylamide) with respect to solvent water, acrylamide, and bisacrylamide; *C*, weight percentage of cross-linker (bisacrylamide) with respect to monomers (acrylamide and bisacrylamide); T*x*C*y*, polyacrylamide gel composed of *x*% *T* and *y*% *C*; TEMED, tetramethylethylenediamine; MPTS, 3-methacryloxypropyl-trimethoxysilane; DMPC, L-α-dimyristoyl-phosphatidylcholine; NBD-DMPE, *N*-(-7-nitro-2–1,3-benzoxadiazol-4-yl)-dimyristoyl-phosphatidylethanolamine; MKS, foot-and-mouth disease (Maul-Klauenseuche); MKS-LP, model lipopeptide carrying the foot-and-mouth disease (Maul-Klauenseuche) virus epitop VP1 135–154 conjugated to the lipotripeptide tripalmitoyl-*S*-glyceryl-cysteinyl-seryl-serine; FITC, fluorescein isothiocyanate; CF, carboxy fluorescein; π, lipid layer transfer pressure; T_t, lipid layer transfer temperature.

0006-3495/94/07/217/10 $2.00

mimic the membrane protein interaction with the polymeric network of the cytoskeleton or the pericellular matrix.

MATERIALS AND METHODS

Lipids

All lipid layers were prepared with L-α-dimyristoyl-phosphatidylcholine (DMPC; Sigma, Deisenhofen, Germany). The fluorescent lipid probe *N*-(-7-nitro-2–1,3-benzoxadiazol-4-yl) L-α-dimyristoyl-phosphatidylethanolamine (NBD-DMPE) was purchased from Avanti Polar-Lipids (Birmingham, AL). The fluorescein isothiocyanate-labeled Maul-Klauenseuche-lipopeptide (MKS-LP, foot-and-mouth disease lipopeptide) was a gift from Dr. G. Jung and W. Beck (Institute of Organic Chemistry, University of Tübingen, Germany). This model compound (3.4 kDa) is composed of foot-and-mouth disease virus VP1 135–154 antigenic determinant and the lipotripeptide tripalmitoyl-*S*-glyceryl-cysteinyl-seryl-serine (Krug et al., 1989) synthesizied by solid phase peptide synthesis and fluorescently labeled with FITC.

Preparation of polyacrylamide films

Thin films of polyacrylamide (PA) gels of various monomer concentrations measured in terms of weight percent of acrylamide monomer with respect to solvent water were prepared on glass substrates (cover glasses of 2.4 × 2.4 cm^2). The degree of cross-linking was adjusted by addition of appropriate amounts of bisacrylamide. In the following, we denote with T*x*C*y* a gel with a monomer mass fraction of *x*% and a cross-linker to monomer ratio of *y*%.

The coupling of the gel with the glass surface was achieved by depositing the contact mediator 3-methacryl-oxypropyl-trimethoxy-silane (MPTS; Serva, Heidelberg, Germany) onto the substrate. The micro-slides were carefully purified by successive ultra sonification first in a 2% (v/v) aqueous Hellmanex (Hellma, Müllheim, Germany) solution (15 min), then in Millipore water (15 min), and finally in acetone (10 min). The first two steps were followed by rinsing in Millipore water, and the last by drying at 75°C for 45 min. For silanization, the slides were kept for 5–7 min in a 0.2% (v/v) solution of MPTS in a 1:1 (v/v) ethanol/water solution. They were then dried for at least 1 h at 75°C. The quality of the film was tested by observation of the wetting by water (contact angle ≈ 62°). Because of the trivalent hydrolyzing methoxyl groups, it must be pointed out that the silane layer might not be monomolecular. The polymer layers were prepared by the so-called flap-technique (Radola, 1980). Appropriate ratios of acrylamide and bisacrylamide (Serva) were dissolved in Millipore water. To these solutions tetramethylethylenediamine (TEMED; Serva) was added to a final concentration of 1.5 mM and ammonium persulfate (Serva) to a final concentration of 5 mM. 5 μl of the polymerizing solution was deposited onto the silanized slides and spread to a thin layer by putting an anti-adhesion polyester cover sheet (Serva) on top. After polymerization for 2 h, the cover foil was removed under water and the polymer film was annealed for 24 h. Water was exchanged 3–4 times. For hydrated gels with $C > 0$, a typical thickness of 30–40 μm was achieved. For $C = 0$ gels, thickness was below 5 μm, because polymer chains not fixed to the cover glass were washed out by the annealing procedure. To determine the thickness of the gels, we measured the distance of a deposited fluorescence-labeled lipid bilayer from the surface of the cover glass by using a confocal arrangement of the microscope.

Deposition of lipid layers

Lipid monolayers were deposited by the Langmuir-Blodgett technique onto substrates covered with the dry polymer film as described previously (Merkel et al., 1989). The bilayers were formed by horizontal dipping of the sample turned down with its monolayer-covered surface through the monolayer at the air/water interface and then kept under water. The transfer pressure π of the lipid layers was 20 mN/m at room temperature (transfer temperature T_t = 22–24°C) when not stated otherwise.

Fluorescence recovery after photobleaching (FRAP or FPR)

The classic spot-bleaching technique using a uniform circular laser beam (Axelrod et al., 1976) was applied for the diffusion measurements. The FRAP apparatus was essentially as described previously (Merkel et al., 1989). The fluorescence recovery after the bleaching pulse is analyzed by the following equation (Soumpasis, 1983)

$$F(t) = F(\infty) - \{F(\infty) - F(0)\} \cdot \left\{1 - e^{-2\tau/t}\left[I_0\left(\frac{2\tau}{t}\right) + I_1\left(\frac{2\tau}{t}\right)\right]\right\} \quad (1)$$

where t is the time after the end of the bleaching pulse ($t = 0$) and $F(t)$ is the fluorescence intensity at time t integrated over the bleaching spot size. I_0 and I_1 are spherical Bessel Functions of 0th and 1st orders. The characteristic fluorescence recovery time t and the relative fluorescence recovery, R, defined by

$$R = \frac{F(\infty) - F(0)}{F_0 - F(0)} \quad (2)$$

(F_0 fluorescence intensity before bleaching) are evaluated by fitting the theoretical to the experimental curves. The diffusion coefficient is defined as

$$D = \frac{r^2}{4\tau} \quad (3)$$

where r is the radius of the bleaching spot.

In some experiments, it has been necessary to correct the measured diffusion coefficients for the systematic error caused by the onset of fluorescence recovery before the end of the bleaching pulse. This leads to an increase of the effective radius of the bleaching spot according to

$$r_{eff} = r + \sqrt{4D_{corr} \cdot t_b}, \quad (4)$$

where t_b is the duration of the bleaching pulse and the corrected diffusion coefficient. The corrected diffusion coefficient is related to the measured value of D, obtained by the fitting procedure, as

$$\frac{D_{corr}}{D} = \frac{r_{eff}^2}{r^2}. \quad (5)$$

Therefore, one obtains

$$D_{corr} = D \cdot \left(1 - \sqrt{\frac{t_b}{\tau}}\right)^{-2}. \quad (6)$$

The validity of the correction has been experimentally checked with a bilayer deposited onto argon sputtered glass. It was found that for $t_b/\tau < 0.2$, the systematic error of the measured diffusion coefficients is smaller than the statistical error.

Measuring chamber

The samples with deposited lipid monolayers were studied in contact with air under high humidity conditions. The bilayer-covered substrates were kept below water. Fig. 1 shows the measuring chamber. To establish high humidity, the lower part of the trough is filled with water and sealed with a wet filter paper and a glass plate. We estimate that the relative humidity under the high humidity condition was greater than 98%, because small water droplets appeared at the rim of the microscope slide above the cover glass (see Fig. 1). No such droplets were observed directly on the sample or at the microscope slide near the measuring region.

For the bilayer experiments, we used a similar trough. The cover glass, including its deposited bilayer facing the interior of the trough, is fixed by silicone grease to the trough. The trough is completely filled with water. Another bilayer setup was to place the cover glass with silicone grease over the water-filled well of a deep-well microscope slide (Merkel et al., 1989). Here the temperature could be controlled via a peltier cooling element attached to the microscope slide.

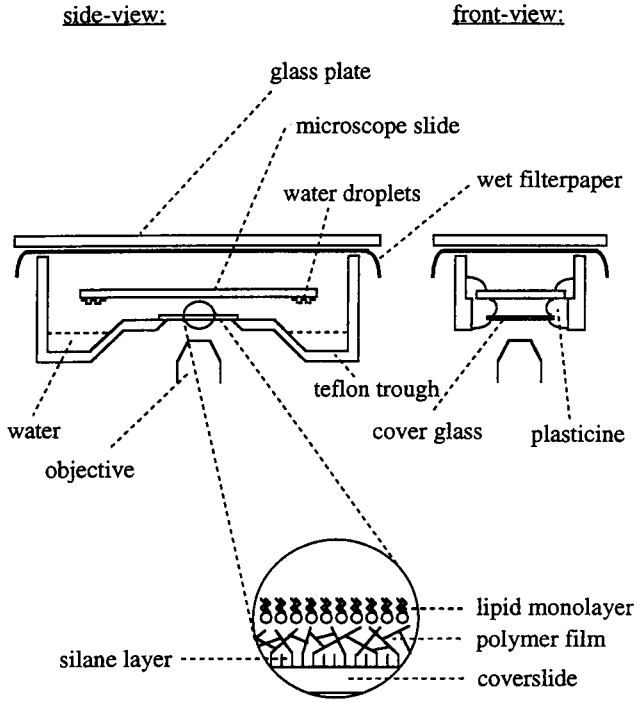

FIGURE 1 Schematic view of the measuring chamber for the monolayer experiments; all view sections include the optical axis. (*inset*) Scheme of the lipid monolayer-polymer-compound system (arbitrary scale).

RESULTS

Lipid monolayers on polymeric films

The Langmuir-Blodgett deposition of the lipid monolayer onto the substrate can be characterized by the transfer ratio, the ratio of the area decrease of the monolayer on the film balance to the area of the cover glass. For all gel supports, T*x*C*y*, x = 5, 10, 20, y = 1, 5, and T20C0, a transfer ratio of 1–1.3 is observed. This indicates a complete wetting of the substrate by the monolayer. In contrast, the transfer ratio of the pure silanized cover glass is 0.05.

Fig. 2 *A* shows a representative fluorescence micrograph of a deposited monolayer at high humidity. The homogeneous fluorescence distribution indicates continuity of the lipid film on a micrometer scale. Fig. 2 *B* presents measurements of the lateral diffusion coefficient, D, of an NBD-DMPE fluorescent probe in a DMPC monolayer deposited onto PA-gels of various compositions at high humidity. Each point corresponds to a measurement at a different site on the monolayer. The diffusion coefficients are corrected for the onset of diffusion during the bleaching pulse. In all cases of Fig. 2 *B*, the recovery, R, is 0.97 ± 0.05 (data not shown). As shown in Figs. 2 *C* and 3, the average lateral mobility depends on the time of annealing, t_{an}, of the gel in the high humidity atmosphere. Thus, for the case of the T20C0-gel support, D increases by a factor of two upon increasing t_{an} from t_{an} = 120 min (measurement #1) to t_{an} = 160 min (measurement #11 in Fig. 2 *C*). For t_{an} = 0, that is, at a room humidity of 30–40%, no diffusion of the lipid is observed. To minimize the effect of slightly varying annealing times (t_{an}), the data of Fig. 2 *B* are corrected by division by the annealing time according to $D_{norm} = D_{corr}/t_{an}$ (Fig. 2 *D*). The assumption of linear swelling of the gel with time is justified because the total time of measurements (≈3 h) is smaller than the time of swelling the gel in water (≈10 h, Tanaka and Fillmore, 1979). Fig. 2 *D* demonstrates that, except for the T20C5-gel support, there is a slight but appreciable increase in diffusion coefficient with decreasing degree of cross-linking. No systematic variation with annealing time is found for the fluorescence recoveries.

To compare the direct frictional coupling of different amphiphiles in the monolayer with the substrate, we measured simultaneously the diffusion of NBD-DMPE and of MKS-LP (a 24-amino-acid polypeptide coupled to a lipid anchor; Fig. 3). For this purpose, the diffusion constants are extracted from the fluorescence recovery by fitting a two component diffusion equation (Fig. 3 *A*). For this evaluation, the recovery of the fast component, the NBD-DMPE probe, is assumed to be 1. This is reasonable because the recovery of the NBD-DMPE alone is R = 0.97 ± 0.05 (see above). Again, the values of the diffusion coefficients vary strongly from site to site by about a factor of 10 for the lipopeptide and a factor of 3 for the phospholipid. In part, this variation is caused by fitting with a two-component diffusion. The fit is especially sensitive when both diffusion constants are of the same order increasing the error by a factor of two. However, the average diffusion coefficient of the lipopeptide is clearly smaller than that of the phospholipid by about a factor of five. The diffusion coefficients of NBD-DMPE in Fig. 2 *B* (only one diffusing fluorophore) and those in Fig. 3 *A* (two diffusing fluorophores) are of same order of magnitude. The spread of the diffusion coefficients for both fluorophores conceals any differences between the different gel supports. Similar to the case of the NBD-DMPE probe in Fig. 2 *D*, the diffusion coefficients of the lipopeptide increase with decreasing degree of cross-linking. Fig. 3 *B* shows that the immobile fraction of MKS-LP increases strongly with increasing monomer and cross-linker concentration. This suggests that the large hydrophilic group of the lipopeptide is subjected to a larger friction by direct coupling to the gel. Analogous to the result of Fig. 2 *C*, the dependence of the mobility on annealing time t_{an} is demonstrated in Fig. 3 where D- and R-values are shown for $t_{an} \approx$ 2 h and $t_{an} \approx$ 6 h both for the phospholipid and the lipopeptide probe. In particular, the ratio of the average D-value of the lipid probe to the lipopeptide probe decreases from a factor of ≈10 at $t_{an} \approx$ 2 h to a factor of ≈3–4 at $t_{an} \approx$ 6 h.

Lipid bilayers on polymeric films

To evaluate the quality of the supported lipid bilayer, different macroscopic features of the DMPC layer are studied, including the homogeneity of the fluorescence of the fluorophore-labeled layers, the width and transition temperature of the phase transition, and the permeability of the bilayers.

Fig. 4, *A* and *B* show representative fluorescence images of a DMPC bilayer deposited onto a T20C0-gel (*A*) and a T20C1-gel (*B*), respectively. The fluorophore NBD-DMPE

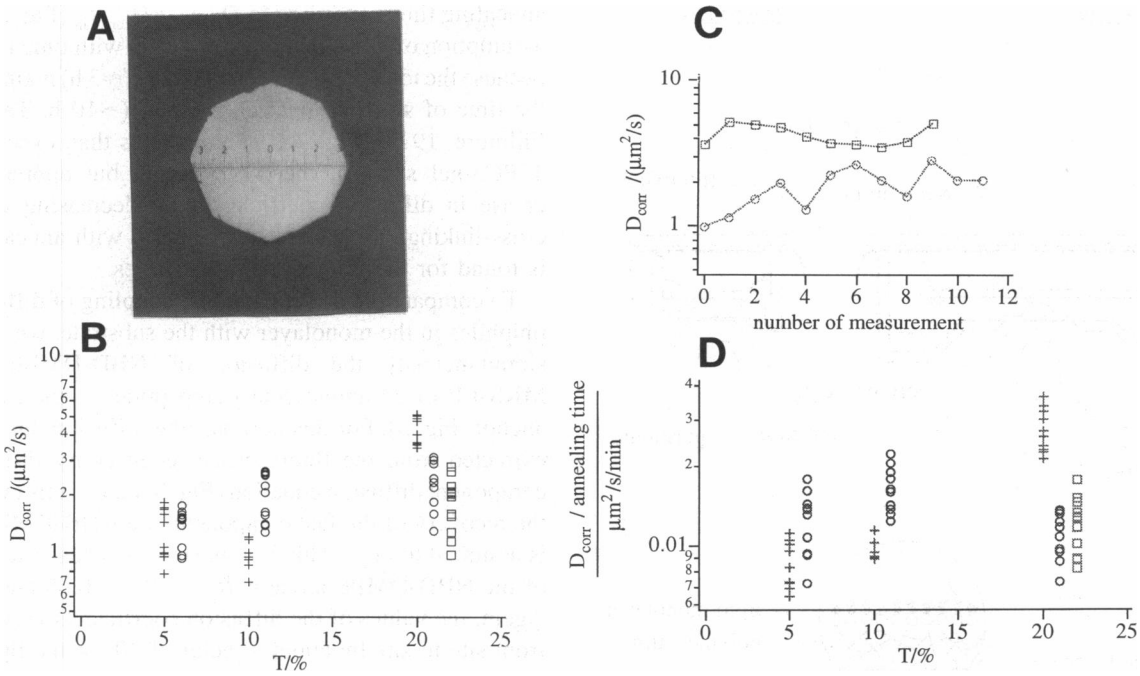

FIGURE 2 (*A*) Fluorescence micrograph of a NBD-DMPE (1 mol%)-labeled DMPC-monolayer deposited onto a T20C0-gel at $T = 21°C$ and high humidity (>98%). The monolayer was transferred at a lateral pressure of $\pi = 20$ mN/m at a transfer temperature of $T_t \approx 15°C$. Distance between numbered ticks is 13 μm. (*B*) Comparison of the lateral diffusion coefficients of NBD-DMPE (1 mol%) in a DMPC monolayer on polyacrylamide gels of three monomer concentrations ($T = 5$, 10, and 20) plotted along the horizontal axis and three cross-linker to monomer mass ratios (+, C5; ○, C1; □, C0). Transfer pressure was $\pi = 20$ mN/m at $T_t \approx 22$–$24°C$, measuring temperature $T = 26°C$, after annealing for about 2 h at high humidity. The data for various C-values are mutually shifted horizontally to avoid overlap. Each point corresponds to a measurement at a different location on the monolayer. Diffusion coefficients are corrected as mentioned in the text. The relative recovery is 0.97 ± 0.05 for all of the gels (data not shown). (*C*) The diffusion coefficient from *B* as function of annealing time given by the number of the measurement under high humidity. Gel composition: □, T20C5; ○, T20C0. (*D*) Normalization of the diffusion coefficients of *B* (D_{corr}/t_{an}) with respect to annealing times, t_{an}, using the data of *B*. A linear swelling with time is assumed. Gel composition: +, C5; ○, C1; □, C0.

(1 mol%) is incorporated in the lipid layer adjacent to the polymer film (proximal layer). The remarkable difference between the images is that the former exhibits a pronounced domain like structure, whereas the latter is homogeneous. No difference is seen when the opposite leaflet (distal layer) is labeled or when images are taken below and above the chain-melting transition temperature. This shows that the bilayer on the non-cross-linked polymer film is heterogeneous and cannot be restored by heating.

The temperature dependence of the lateral diffusion coefficient of a NBD-DMPE probe shows an increase of *D* at 22.5 ± 2.5°C for the T20C0- and the T20C1-sample, indicating a bilayer phase transition (Fig. 4 *C*). Although a relatively sharp increase in *D* is found for T20C0, the increase for T20C1 is more continuous. Moreover, the diffusion coefficients for the C1-system are larger than for the C0-sample. Within the experimental accuracy, the recovery does not depend on temperature. However, all of the recovery values for the C0-system (0.78 ± 0.11) are smaller than those of the C1-sample (0.93 ± 0.1). Together with the homogeneous fluorescence, this strongly suggests that the lipid layer on the cross-linked polymer is more continuous.

To test for leaks in the DMPC-bilayer deposited on a T20C1-gel, we measured the diffusion of the membrane-impermeable fluorescent probe carboxy fluorescein from the bulk buffer through the bilayer into the polymer gel. One hour after addition of carboxy fluorescein to the bulk buffer, the variation of the fluorescence intensity was measured as a function of the height above the cover glass in a confocal set-up of the microscope (Fig. 5 *A*). The data (*circles*) are fitted to a theoretical intensity profile, which is evaluated as a convolution of a theoretical fluorophore distribution and the detection function of the optical system. Assuming the fluorophore distribution shown in Fig. 5 *B*, which accounts for the different fluorophore concentrations in the gel and in the buffer above the gel, this fit (*line* in Fig. 5 *A*) shows that the main rise in fluorescence occurs at the position of the glass surface ($d_0 \approx 0$). Thus, the bilayer is permeable despite the rather homogeneous fluorescence distribution of the Fig. 4 *B*. This fit further reveals a gel thickness of about $d_1 \approx 40 \pm 3$ μm.

For possible use in biosensor technology, the diffusion of a lipid-linked antigen epitope, MKS-lipopeptide (MKS-LP), is considered. Table 1 reveals an immobile fraction of MKS-LP (1 mol%) for both leaflets of a DMPC bilayer on a T20C1-gel. Although the diffusion coefficient of the MKS-LP molecule in the proximal leaflet is significantly smaller than in the distal one, both are smaller than 8 μm²/s, the diffusion coefficient of NBD-DMPE at $T = 30°C$ in both leaflets (Fig. 4 *C*).

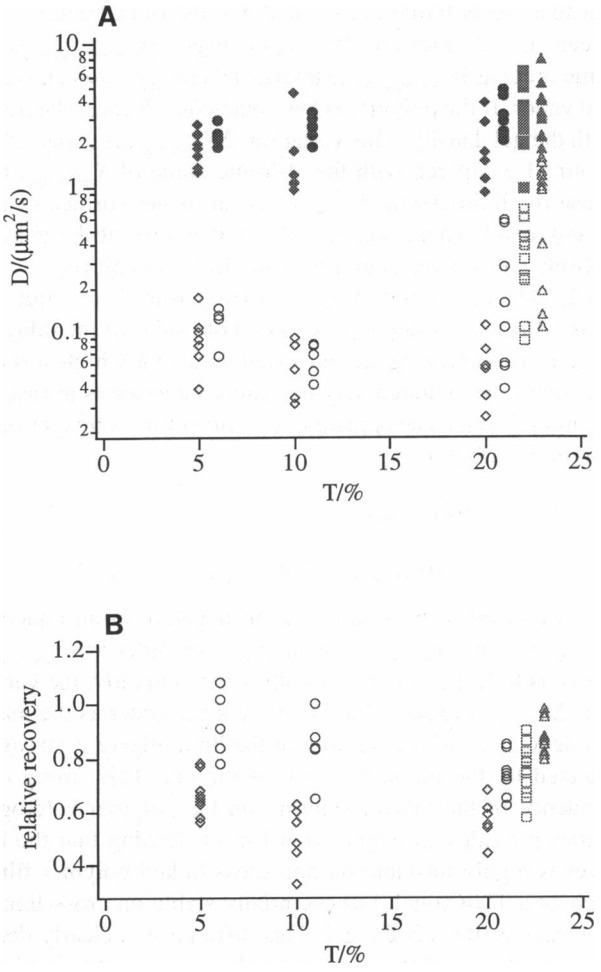

FIGURE 3 (*A*) Simultaneous diffusion measurements of 1 mol% NBD-DMPE (*closed symbols*) and 1 mol% MKS-LP (*open symbols*) in a DMPC monolayer (π = 20 mN/m; $T_t \approx$ 22–24°C) for different monomer and cross-linker concentration of the gel. Samples were annealed for 2 or 6 h at high humidity at $T \approx$ 26°C. Gel composition: ◇, ◆, C5; ○, ●, C1; □, ■, C0 (all) ≈2 h annealing time; △, ▲, C0 ≈ 6 h annealing time. (*B*) Fluorescence recovery of MKS-LP of the simultaneously measured diffusion of 1 mol% NBD-DMPE and 1 mol% MKS-LP in a DMPC monolayer for different monomer and cross-linker concentration of the gel (π = 20 mN/m; $T_t \approx$ 22–24°C). Samples were annealed for 2 or 6 h at high humidity at $T \approx$ 26°C. A recovery of one is assumed for the NBD-DMPE fluorophore. ◇, C5; ○, CA; □, C0, all ≈2 h annealing time; △, C0 ≈ 6 h annealing time.

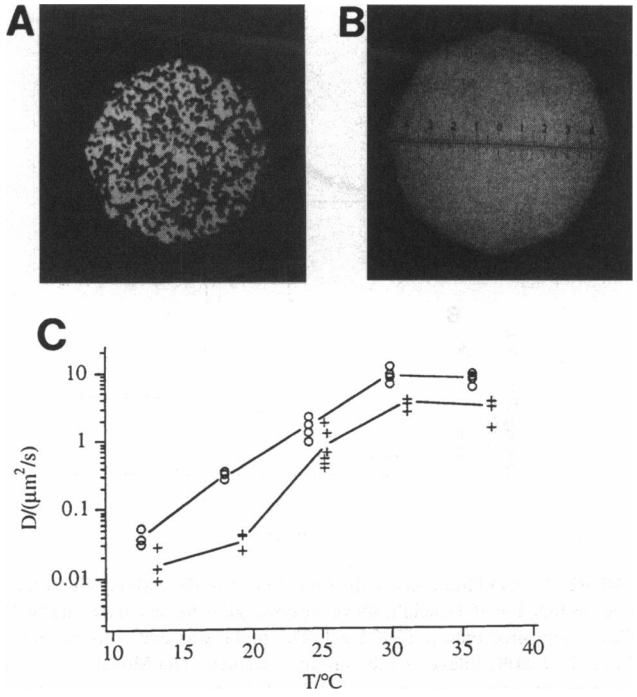

FIGURE 4 (*A*, *B*) Fluorescence images of a DMPC bilayer deposited onto a T20C0-gel (*A*) and a T20C1-gel (*B*). The lipid fluorophore NBD-DMPE is incorporated in the lipid layer adjacent to the polymer film (proximal leaflet). Images were taken at T = 12°C, but no difference is seen for $T >$ 25°C. (π = 20 mN/m; T_t = 22°C; distance between numbered ticks is 13 μm.) (*C*) Temperature dependence of lateral diffusion coefficient of NBD-DMPE-probe (1 mol%) in proximal leaflet of DMPC bilayer deposited on different gels; +, T2OC0; ○, T2OC1 (π = 20 mN/m; $T_t \approx$ 22°C). Within the accuracy of measurement, no temperature dependence of the recovery, R, for either gel support is observed. R(T20C0) = 0.78 ± 0.11; R(T20C1) = 0.93 ± 0.10.

DISCUSSION

Composite, supported films composed of lipid layers supported by a polymer film are of particular interest for functionalization of solid surfaces and the reconstitution of membrane spanning proteins into the fluid bilayer in such a way that denaturation is avoided. Considering such applications, several questions are of interest. How continuous and stable is a lipid layer on a polymer film, which is not directly coupled to the support by covalent linkage or via charged polymers? How are the structural, thermodynamic, and dynamic properties of the lipid layer affected by the polymer? What can we learn about the polymer-lipid interface and the interaction between the polymer network and lipid layer? In the first part of the discussion, we focus on the stability problem and address the question of whether it is possible to deposit stable lipid layers on polymer gels. In the second part, we discuss aspects of the monolayer-polymers interface in more detail, and in the third part, we deal with the bilayer-polymer system.

Polymer heterogeneity, hydration, and lipid layer stability

If we consider the polymer film as a semidilute solution, its mesh size, ξ, is of the order (de Gennes, 1979)

$$\xi \sim a \cdot \varphi_P^{-3/4}, \tag{7}$$

where a is the monomer diameter and the polymer volume fraction, which is approximately equal to the monomer concentration T ($T \approx \varphi_P$). Because $a \approx$ 0.5 nm, the mesh size should be of the order $\xi \approx$ 5 nm for the T5 and $\xi \approx$ 2 nm for the T20-system, and the polymer film should be smooth on a 10-nm scale. However, our finding that the variation of the diffusion coefficient (50% for NBD-DMPE in monolayers on T20C0, Fig. 2 *B*) and the fluorescence recovery of the mono- and bilayer on the polymer is greater than the measuring error (10% for the diffusion coefficient) suggests that

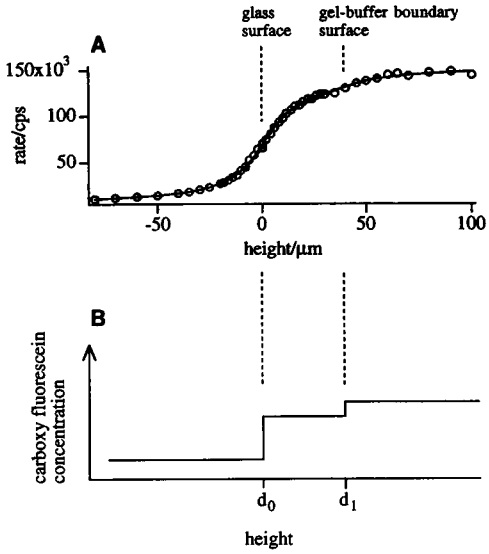

FIGURE 5 (*A*) Fluorescence distribution (○) of the carboxy fluorescein probe as function of the height above the cover glass for an unlabeled DMPC bilayer deposited onto a T20C1-gel. The probe was added to the buffer above the DMPC bilayer 1 h before measurement. (*B*) Model of the distribution of the fluorescent probe over the glass surface. d_0: vertical position of the glass surface; d_1: position of the lipid bilayer. To evaluate the theoretical intensity distribution, this concentration profile is convoluted with the detection function of the optical system. A fit (line in *A*) of this theoretical intensity distribution to the data in *A* reveals a gel thickness of about 40 μm.

TABLE 1 Diffusion coefficient of MKS-LP

	D (μm²/s)	R
MKS-LP (1%), proximal label	1–2 (1.4)	0.60–0.80 (0.68)
MKS-LP (1%), distal label	4–6 (4.7)	0.72–0.87 (0.82)

Diffusion coefficient of MKS-LP (1mol%) in each leaflet of a DMPC bilayer deposited on T20C1-gel at T = 30°C in millipore water (Transfer pressure π = 20 mN/m, transfer temperature T_t = 24°C. Range and average (parentheses) values are shown).

both types of lipid layers are inhomogeneous. The inhomogeneity of the lipid layers might be caused by a heterogeneity of the polymer film. Evidence for this effect is provided by our observation that monolayers show homogeneous fluorescence images. They are thus stable and continuous on the cross-linked and non-cross-linked gels, whereas bilayers do so only for cross-linked gels ($T = 20$, $C > 0$). To understand why the stability of bilayer is more affected by the gel inhomogeneity than that of the monolayer, we consider two cases:

(1) Monolayer supported by a polymer film at high humidity (>98%). The homogeneity of the fluorescence distribution strongly suggests that the monolayer is stable and continuous, showing that the monolayer readily spreads on the polymer film. The stability of the lipid layer is determined by the spreading coefficient $S_{\text{monolayer}}$, the difference between the interfacial energies, σ_{ij}, of a substrate, which is not covered with a monolayer, and of a substrate that is covered with a layer. It is

$$S_{\text{monolayer}} = \sigma_{\text{polymer,vapor}} - (\sigma_{\text{polymer,lipid}} + \sigma_{\text{lipid,vapor}}) > 0. \quad (8)$$

Because the polymer is hydrated, the interfacial energy between the polymer and the vapor phase, $\sigma_{\text{polymer,vapor}}$, is of same order as $\sigma_{\text{water,vapor}}$, the interfacial energy between water and vapor. If the polymer is heterogeneous, S varies laterally with the gel density. This variation, $\Delta S_{\text{monolayer}}$, is expected to be small compared with the absolute value of $S_{\text{monolayer}}$, because the lipid essentially wets the air/water surface of the hydrated gel. Therefore, the inhomogeneities of the gel are not relevant for the stability of the lipid monolayer.

(2) Bilayer supported by a polymer film in an aqueous phase. Because water is present on both sides of the bilayer, there is no stabilizing effect caused by the very high surface tension of the hydrated polymer-vapor interface as in case of the monolayers. The spreading coefficient for a bilayer on a polymer surface is

$$S_{\text{bilayer}} = \sigma_{\text{polymer,water}} - (\sigma_{\text{polymer,lipid}} + \sigma_{\text{lipid,lipid}} + \sigma_{\text{lipid,water}}). \quad (9)$$

It is expected to be small or even negative in an aqueous phase, because $\sigma_{\text{polymer,water}}$ is of the same order as $\sigma_{\text{water,water}}$, which is 0. If the polymer density varies laterally, the variation $\Delta S_{\text{bilayer}}$ is expected to be of the same order as the magnitude S_{bilayer}, and the stability of the lipid bilayer is strongly affected by the inhomogeneity of the gel. This strong dependence of the bilayer stability on the polymer heterogeneities provides an explanation for our finding that the bilayer is highly unstable on non-cross-linked polymer films such as a T20C0-gel, but essentially stable on cross-linked gels such as the T20C1-gel. This difference is clearly demonstrated by the difference of the fluorescence distributions shown in Fig. 4, *A* and *B* and by the finding that the fluorescence recovery is much smaller than one (namely, $R = 0.78 \pm 0.11$) for DMPC-bilayers on T20C0-gels, but is nearly one ($R = 0.93 \pm 0.1$) on T20C1-gels.

The inhomogeneity of the polymer layers can have the following origin: (i) heterogeneous grafting of the polymer to the support, resulting in a heterogeneous polymer distribution and exposure of the silanated glass surface to the lipid layer, or (ii) local segregation or micro-gelation of the polymer into clusters of high and low polymer density, which is relevant for both the non-cross-linked and the chemically cross-linked polymer film. In case of the T20C0-gel, heterogeneous grafting is relevant because of the small thickness of the polymer film (<5 μm). As a reason for patterned fluorescence polymer-induced domain formation is unlikely (a) because the pattern does not change when the sample is heated to 50°C, and (b) because no pattern is observed for the T20C1-gels.

Frictional coupling between lipid monolayers and polymeric films

In this section, we consider the monolayer supported by a polymer film more carefully. As mentioned above, the diffusion coefficient of NBD-DMPE is smaller for a gel-supported monolayer than for a free, uncoupled monolayer

at the water surface. This slowing down is attributed to the frictional coupling of the monolayer to the polymer.

If a fluid lipid layer is coupled to a rigid surface by a thin lubricating layer (thickness h), the classical Saffman-Delbrück theory has to be modified by considering the frictional tension, σ, generated by the friction between the lipid layer and the solid surface, which is given by

$$\sigma = \eta_w \frac{v}{h} = b_s \cdot v, \tag{10}$$

where η_W is the water viscosity, v is the momentary velocity of the diffusant, and b_s is the frictional coefficient (Evans and Sackmann, 1988). The diffusion coefficient can be expressed as a function of a normalized radius of the diffusant,

$$D = \frac{kT}{4\pi\eta_m} \cdot \frac{1}{\frac{1}{4}\epsilon^2 + \epsilon\frac{K_1(\epsilon)}{K_0(\epsilon)}},$$
$$\epsilon = a_p \cdot \sqrt{\frac{\eta_w}{\eta_m h}} = a_p \cdot \sqrt{\frac{b_s}{\eta_m}}, \tag{11}$$

where a_p is the Van der Waals radius of the diffusant and η_m is the lipid layer viscosity. K_0 and K_1 are modified Bessel Functions of the second kind of order 0 and 1. Depending on ϵ, one can discuss two limiting cases. For the weak coupling case ($\epsilon \ll 1$), the classical Saffman-Delbrück law holds

$$D = \frac{k_B T}{4\pi\eta_m} \ln\left(\frac{1}{\epsilon}\right). \tag{12}$$

For strong-coupling $\epsilon \gg 1$, one gets

$$D = \frac{k_B T}{\pi b_s a_p^2} = \frac{k_B T h}{\pi \eta_w a_p^2}. \tag{13}$$

In this case, D is strongly dependent on the size of the diffusant and the thickness, h, of the coupling layer. For diffusants in the proximal layer with large hydrophilic groups penetrating far into lubricating water film, b_s is determined by the direct coefficient of friction exerted on the hydrophilic group.

In Table 2, a number of frictional coefficients are given. The apparent frictional coefficient, b_s, of NBD-DMPE in a gel-supported monolayer exceeds the corresponding value on a free water surface by at least three orders of magnitude. Hence, the water film between lipid layer and the polymer film should be of molecular thickness. For a given gel composition, the apparent frictional coefficient of the MKS-lipopeptide (Table 2) is greater than that of the NBD-DMPE, thus indicating a larger hydrophilic group penetrating into the gel.

We will focus on the MKS-LP in the further discussion because the differences between different gels seem to be more pronounced. For the T20Cx-sample, an increasing diffusion coefficient and an increasing fluorescence recovery is observed for the MKS-lipopeptide (MKS-LP) molecule (Fig. 3) with decreasing degree of cross-linking. In particular, for the C1-gel the recovery of MKS-LP is well below 1

TABLE 2 Summary of diffusion coefficients

DMPC monolayer with different fluorophores and supports	D ($\mu m^2/s$)	b_s (dyn s/cm^3)
NBD-DMPE,* air-water interface on film balance, free layer (Meller, 1985)	13	330
NBD-DMPE, T20C0, T20C1	1–3 (2)	$8.8\cdot10^6$–$1.5\cdot10^8$ ($3.2\cdot10^7$)
NBD-DMPE, T20C5	3.5–5	10^6–$5\cdot10^6$
MKS-LP, T20C0	0.1–1	$6.8\cdot10^7$–$2.3\cdot10^9$
MKS-LP, T20C1	0.04–0.7	$1.3\cdot10^8$–$6.8\cdot10^9$

Summary of diffusion coefficients and frictional coefficient of lipid and lipopeptide probe in a DMPC monolayer on different supports after annealing for about 2 h at high humidity (≈98%). The transfer pressure was π = 20 mN/m and the transfer temperature $T_t \approx$ 22°C. The measuring temperature was T = 26°C except for *, where the measuring temperature was 20°C. For the evaluation of the frictional coefficient according to Eq. 11, the following parameters are used; bilayer intrinsic membrane viscosity: $\eta_m(T = 26°C) = 1.6\cdot10^{-7}$dyn s/cm; radius of the lipid in the lipid layer: a_p(DMPC) ≈ 4 Å (Merkel et al., 1989); radius of the lipid anchor of the lipopeptide in the lipid layer: a_p(MKS-LP) ≈ 6 Å. Range and average (parentheses) values are shown.

and is remarkably small for the C5-gel. The partial immobilization in the gel clusters is an indication of direct coupling of lipopeptide with the substrate.

The decrease of diffusion coefficient of the MKS-LP with increasing cross-linking might have different reasons. (1) In a first approach, the surface is considered as homogeneous, and an effective frictional coefficient is evaluated (Table 2). Increasing the cross-linker concentration decreases the elasticity and increases the surface viscosity of the polymer and, thus, increases the friction. (2) In a second approach, the decrease of diffusion coefficient can be explained by the heterogeneity of the polymer. In terms of the micro-gelation model, the monolayer is composed of regimes with strong and weak frictional coupling, characterized by large (D_f) and small (D_s) diffusion coefficients. This situation can be described by the effective diffusion model proposed by Saxton (1982) on the basis of the Bruggeman-Landauer equation,

$$D^* = \frac{D_f(c)}{D_s(c=0)}$$
$$= (c - \tfrac{1}{2})(1 - r) + \sqrt{(c - \tfrac{1}{2})^2(1 - r)^2 + r}, \tag{14}$$

where D^* is the "composed," measured diffusion coefficient, $r = D_s/D_f$, and c is the area fraction exhibiting strong coupling. The data of Fig. 3 can be interpreted in terms of this model by assuming that the diffusion within the strongly coupled domains can be ignored on the time scale of the measurement. In this case, $c \approx 1 - R$, where R is the relative fluorescence recovery. In Fig. 6, the Bruggeman-Landauer curve is fitted to the data for the T20Cx-gels, yielding a value of $D_s/D_f \approx 0.005$. To estimate the frictional coefficient in the weak coupling areas, we extrapolate to $R = 1$. This leads to a diffusion constant of $D(c = 0) = 0.65$ $\mu m^2/s$ and a friction coefficient of $1.5\cdot10^8$ dyn s/cm^3, assuming a radius of 6 Å of

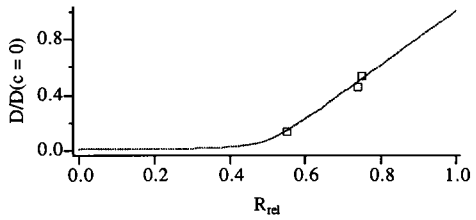

FIGURE 6 Impediment of the diffusion of MKS-lipopeptide embedded in a monolayer at high humidity caused by micro gelation of the polymer surface. The dependence of the normalized diffusion coefficient is shown as a function of the fluorescence recovery, which is a measure for the mobile area fraction of the probe. The data (□) are fitted (*line*) to the effective medium theory, discussed in the text, which relates the normalized diffusion coefficient to the immobile area fraction c. On the time scale of the experiment $c \approx 1 - R$.

the lipid anchor of MKS-LP molecule in the membrane. This is by a factor of 5 greater than the b_s-value of NBD-DMPE ($D = 2\ \mu m^2/s$, $b_s = 3.2 \cdot 10^7$ dyn s/cm^3), indicating a greater friction caused by the larger hydrophilic group even in the weakly coupled areas. For the NBD-DMPE probe, the difference between measured, effective ($D(c > 0, R < 1)$) and physical ($D(c = 0)$) diffusion coefficient is not significant because the recovery is almost one.

The decrease in recovery with increasing cross-linker ratio at constant monomer ratio T or with increasing monomer fraction at constant cross-linker ratio C can also be explained in terms of the micro-gelation of the polymer: in both cases, the actual cross-linker concentration increases, which is expected to lead to a higher area fraction covered by strong-coupling gel surfaces. On these, the recovery is negligibly small.

Lipid bilayers on polymeric films

The permeability of the bilayer to carboxy fluorescein (CF) on a time scale of 1 h shows that the bilayer is not continuously closed, because vesicles are practically impermeable to CF-fluorophore diffusion (Fraley et al., 1981; Tampé and Galla, 1991). Two models of leakage of the bilayer on the gel are considered. First, the leakage can be caused by small holes or defects, and CF diffusion is essentially perpendicular to the lipid layer (one-dimensional diffusion). From the time scale of fluorescence increase ($t \approx 500$ s) in the polymer region (thickness $d \approx 40\ \mu m$) at the center of the sample, when the bulk buffer is mixed with CF, one can calculate an effective diffusion coefficient, $D = d^2/2t \approx 2\ \mu m^2/s$). This is at least a factor of 100 smaller than what is expected for CF in polyacrylamide ($D_{CF} \geq 500\ \mu m^2/s$). Second, CF penetrates into the gel at larger holes or scratches, which are observed at least at the rim of the polymer film. Then it diffuses through the polymer gel to the center of the sample, where it increases the fluorescence intensity in the polymer region. For this two-dimensional diffusion, a mean separation of the scratches $\Delta = \sqrt{4D_{CF}t} \approx 1$ mm can be estimated. Taking into account the not quite homogeneous fluorescence of the bilayer (Fig. 4 *B*), the first model is more likely.

Although the permeability of the bilayers to carboxy fluorescein shows that the bilayers are heterogeneous, other properties of the lipid layer on the polymer substrates are similar to those of DMPC-vesicles. In the following, we summarize several properties indicating that the bilayer on the T20C1-gel is only slightly disturbed as compared with the free DMPC bilayer.

(1) The diffusion coefficient of the NBD-DMPE probe in the lipid layer on the T20C1-gel ($D \approx 6$–$10\ \mu m^2/s$, $T = 30°C$) are higher than those on argon-sputtered cover glass ($D \approx 3$–$4\ \mu m^2/s$, $T = 30°C$), indicating a smaller coupling (see b_s in Table 3) to the gel than to the sputtered glass. The D-value agrees well, however, with the value in multibilayer systems ($D \approx 8\ \mu m^2/s$, $T = 30°C$; Wu et al., 1977), showing that the lipid layer is nearly undisturbed. The diffusion coefficients of the lipid probe on the T20C0-gel is lower than on the T20C1-gel ($D \approx 3$–$4\ \mu m^2/s$ compared with $D \approx 6$–$10\ \mu m^2/s$ for $T \approx 30°C$) because of the patched fluorescence distribution: to reach the bleached area, the fluorophores have to diffuse through many bottlenecks, which slows down the recovery process, and a "composed" diffusion coefficient is measured.

(2) Another important property of DMPC-bilayers is the chain-melting transition. Fig. 4 *C* indicates a phase transition temperature at $T_t \approx 22°C$, similar to the value for DMPC bilayers on argon-sputtered glass (Merkel et al., 1989), on oxidized silicon wafer (Tamm and McConnell, 1985), and of DMPC multibilayers (Wu et al., 1977).

Surface viscosity of polymeric films

The MKS-lipopeptide in a lipid bilayer deposited on a T20C1-gel can be considered as a model of a protein in the plasma membrane, the diffusion of which is impeded by the coupling of the hydrophilic part of the protein to the extracellular matrix or the membrane-bound cytoskeleton. In analogy to the protein diffusion in most cell membranes (see, for example, Golan and Veatch, 1980), the lipopeptide molecule shows a remarkable immobile fraction (Table 1). This might be because of aggregation of lipopeptides into greater particles, which would provide an explanation for the low fluorescence recovery of the lipopeptides embedded in the outer (distal) monolayer. Strong coupling of the molecules to the high density areas of the gel might also be relevant because a remarkable increase in fluorescence recovery from 0.6 ± 0.07 at 30°C to 0.92 ± 0.08 at 45°C is observed. The reasons for the lower diffusion coefficients of the MKS lipopeptide compared with the lipid probe are the same as in case of the monolayer: the diffusion coefficient might be a "composed" diffusion coefficient or the friction is increased because of the larger size of the MKS lipopeptide. Provided the first reason can be neglected, we take two different points of view:

(1) The surface viscosity of the polymer film can be estimated from the difference of the diffusion coefficients of lipopeptide (LP) in the proximal and distal lipid layer as follows. In a simple model, one can add up all the frictional

TABLE 3 Diffusion and fractional coefficient of fluorophores

DMPC bilayer with different fluorophores and supports	D ($\mu m^2/s$)	b_s (dyn s/cm^3)
NBD-DMPE, argon sputtered glass, proximal or distal labeled	3–4 (3.4)	$2.7 \cdot 10^5$–$1.5 \cdot 10^6$
NBD-DMPE, T20C0, proximal- or distal-labeled	2–4 (3.1)	$2.7 \cdot 10^5$–$9.2 \cdot 10^6$
NBD-DMPE, T20C1, proximal- or distal-labeled	6–10 (7.1)	7–$8.5 \cdot 10^4$
MKS-LP, T20C1, proximal-labeled	1–2 (1.4)	$4.1 \cdot 10^6$–$3.5 \cdot 10^7$ ($1.4 \cdot 10^7$)
MKS-LP, T20C1, distal-labeled	4–6 (4.7)	$3.8 \cdot 10^3$–$1.2 \cdot 10^5$ ($3.8 \cdot 10^4$)

Diffusion and frictional coefficient (D and b_s) of various fluorophores in DMPC bilayer on different supports at $T = 30°C$. The transfer pressure was $\pi = 20$ mN/m, the transfer temperature $T_t \approx 23$–$24°C$. For the evaluation of the frictional coefficient according to Eq. 13, the following parameters are used: bilayer intrinsic membrane viscosity: $\eta_m(T = 30°C) \approx 2.8 \cdot 10^{-7}$dyn s/cm; radius of the lipid in the lipid layer: a_P(DMPC) ≈ 4 Å (Merkel et al., 1989); radius of the lipid anchor of the lipopeptide in the lipid layer: a_P(MKS-LP) ≈ 6 Å. Range and average (parentheses) values are shown.

forces (Lee et al., 1993). The friction of the lipopeptide in the proximal leaflet is the sum of the friction of the fatty acid chains in the lipid layer and of the hydrophilic group in the polymer gel:

$$\gamma_{polymer} + \gamma_{layer} = \frac{kT}{D_{LP,proximal}}. \quad (15)$$

An analog consideration yields

$$\gamma_{water} + \gamma_{layer} = \frac{kT}{D_{LP,distal}} \quad (16)$$

for the outer leaflet. The Stokes-Einstein law leads to the following equation for the viscosity difference of the water and the gel, respectively.

$$\frac{kT}{D_{LP,proximal}} - \frac{kT}{D_{LP,distal}} = \gamma_{polymer} - \gamma_{water} = 6\pi(\eta_{polymer} - \eta_{water}) \cdot r. \quad (17)$$

Here the hydrodynamic radius, r, of the hydrophilic group and the surface viscosity, $\eta_{polymer}$, of the gel are the only unknown parameters. The radius r may be estimated by comparing the diffusion coefficient of the lipid probe (L) and the lipopeptide probe (LP) in the distal layer. The stronger friction of the lipopeptide molecule is caused both by the greater radius, a_P, of the lipid anchor in the lipid layer (three instead of two fatty acid chains) and the greater radius of the hydrophilic group. Thus,

$$\frac{kT}{D_{LP,distal}} - \frac{kT}{D_{L,equivalent}} = 6\pi \cdot \eta_{water} \cdot r, \quad (18)$$

where $D_{L,equivalent} = 4.9$ $\mu m^2/s$ is the theoretical diffusion coefficient of a molecule with the radius of the lipopeptide in the lipid layer ($a_P \approx 6$ Å) but with a frictional coefficient like a NBD-DMPE molecule, diffusing in the distal lipid layer ($b_s \approx 250$ dyn s/cm^3, assuming an average $D \approx 8$ $\mu m^2/s$). With $\eta_{water} \approx 0.8$ cP, taking the bulk value as an approximation for the viscosity of the water film adjacent to the membrane, $D_{LP,distal} = 4.7$ $\mu m^2/s$, $D_{L,distal} = 8$ $\mu m^2/s$, $D_{LP,proximal} = 1.4$ $\mu m^2/s$, $T = 30°C$, a radius of $r \approx 24$ Å for the hydrophilic group of the MKS-LP molecule and a polymer surface viscosity of 0, 5P is obtained. This value is approximately the same value as the surface viscosity of the pericellular matrix measured by Lee et al. (1993). In that aspect, the polymer film can be a model system for the extracellular matrix.

(2) Another point of view is to evaluate the friction coefficients b_s by the Evans-Sackmann model. In Table 3, the influence of the larger hydrophilic group of the MKS-LP compared with the NBD-DMPE is demonstrated by the increase of the friction coefficient by at least two orders of magnitude. Knowing the friction coefficient b_s and the viscosity of the medium adjacent to the monolayer considered, a typical interaction distance $h = \eta_m/b_s$ can be estimated. For the distal-labeled layer with $\eta_m = \eta_{water} \approx 0.8$ cP and $b_s = 3.8 \cdot 10^4$ dyn s/cm^3 (Table 3), we get $h \approx 21$ Å and for the proximal side ($\eta_m = \eta_{polymer} \approx 0.5P$, $b_s = 1.4 \cdot 10^7$ dyn s/cm^3, Table 3) $h \approx 4$ Å. Although the first value is of the same order as the radius of the hydrophilic part of the lipopeptide (24 Å) estimated in the first approach, the second is significantly smaller. This provides strong evidence that the polypeptide chain of MKS-LP significantly penetrates into the gel.

CONCLUSIONS

In this paper, we showed that lipid monolayers and bilayers can be deposited by noncovalent linkage onto thin polymer films on solid supports without remarkable pertubation of their structural, dynamic, and thermodynamic properties.

Although the deposition of the continuous monolayers exposed to air is rather insensitive towards polymer heterogeneities on a micrometer scale, bilayers below water are much more sensitive and exhibit local dewetting on heterogeneous, non-cross-linked polymer films. In accordance with previous studies on the stability of a polymer-lipid film exposed to a high humidity atmosphere (Elender and Sackmann, 1994), the present study shows that the wetting laws have to be carefully considered for the preparation of supported polymer-lipid composite membranes, which are stable and continuous over macroscopic dimensions (>100 μm). The presented type of model membrane is of particular interest for studies of the friction between membranes and polymer surfaces or to determine the effective viscosity of polymer surfaces. Moreover, a more systematic study of the diffusion of molecular probes with large hydrophilic groups within the two leaflets of a supported bilayer is expected to allow a more quantitative analysis of the heterogeneity of the polymer film. The weak frictional coupling of the lipid layer to the polymer film would allow the undisturbed reconstitution of membrane spanning proteins such as receptors to gain insight into the impediment of diffusion of membrane proteins by their coupling to the cytoskeleton and the extracellular matrix

or by the crowding effect. The separation of the lipid layer from the solid supports by a soft polymer cushion opens new possibilities for the preparation of biocompatible substrates. These supports can enable the undisturbed immobilization of cells to study fundamental aspects of cell adhesion and cell locomotion. These supports can enable the local enrichement of reconstituted membrane-spanning proteins in lipid layers by two-dimensional electrophoresis. These flat membranes can allow more detailed studies of specific recognition, binding, and transport processes by surface-sensitive optical techniques and electrical measurements.

We thank Mr. Christian Dietrich for the help and tips during the monolayer preparations and Dr. G. Jung and W. Beck for the preparation of the foot-and-mouth disease lipopeptide.

This work was supported by the Bundesminister für Forschung und Technologie (BMFT O319431 A).

REFERENCES

Axelrod, D., D. E. Koppel, J. Schlessinger, E. Elson, and W. W. Webb. 1976. Mobility measurement by analysis of fluorescence photobleaching recovery kinetics. *Biophys. J.* 16:1055–1069.

Bayerl, T., and M. Bloom. 1990. Physical properties of single phospholipid bilayers adsorbed to micro glass beads—a new vesicular model system studied by ^{2}H-nuclear magnetic resonance. *Biophys. J.* 58:357–362.

de Gennes, P. G. 1979. Scaling Concepts in Polymer Physics. Cornell University Press, Ithaca, New York.

Elender, G., and E. Sackmann. 1994. Wetting and dewetting of Si/SiO_2-wafers by free and lipid-monolayer covered aqueous solutions under controlled humidity. *J. Phys. II France.* 4:455–479.

Evans, E., and E. Sackmann. 1988. Translational and rotational drag coefficient for a disk moving in a liquid membrane associated with a rigid substrate. *J. Fluid Mech.* 194:553–561.

Fraley, R., R. M. Straubinger, and D. Papahadjopoulos. 1981. Liposome-mediated delivery of deoxyribonucleic acid to cells: enhanced efficiency of delivery related liposome composition and incubation conditions. *Biochemistry.* 20:6978–6987.

Galla, H. J., W. Hartmann, U. Theilen, and E. Sackmann. 1979. On two-dimensional passive random walk in lipid bilayers and fluid pathways in biomembranes. *J. Membr. Biol.* 48:215–236.

Golan, E. G., and W. Veatch. 1980. Lateral mobility of band 3 in the human erythrocyte membrane studied by fluorescence photobleaching recovery: evidence for control by cytoskeletal interactions, *Proc. Natl. Acad. Sci. USA.* 77:2537–2541.

Krug, M., G. Folkers, B. Haas, G. Hess, K. H. Wiesmueller, S. Freund, and G. Jung. 1989. Molecular dynamics of the α-helical epitope of a novel synthetic lipopeptide foot-and-mouth disease virus vaccine. *Biopolymers.* 28:499–512.

Lee, G. M., F. Zhang, A. Ishihara, C. L. McNeil, and K. A. Jacobson. 1993. Unconfined lateral diffusion and an estimate of pericellular martix viscosity revealed by measuring the mobility of gold-tagged lipis. *J. Cell Biol.* 120:25–35.

Meller, P. 1985. Untersuchungen der mikrostruktur und lateral-diffusion in monoschichten aus phospolipiden and polymerisierbaren amphiphilen. Thesis, Technical University Munich.

Merkel, R., E. Sackmann, and E. Evans. 1989. Molecular friction and epitactic coupling between monolayers in supported bilayers. *J. Phys. France.* 50:1535–1555.

Radola, B. J. 1980. Ultrathin-layer isoelectric focusing in 50–100 μm polyacrylamide gels on silanized glass plates or polyester films. *Electrophoresis.* 1:43–56.

Saxton, M. J. 1982. Lateral diffusion in an archipelago—effects of impermeable patches on diffusion in a cell membrane. *Biophys. J.* 39:165–173.

Soumpasis, D. M. 1983. Theoretical analysis of fluorescence photobleaching recovery experiments. *Biophys. J.* 16:95–97.

Stelzle, M., R. Miehlich, and E. Sackmann. 1992. Two-dimensional microelectrophoresis in supported lipid bilayers. *Biophys. J.* 63:1346–1354.

Stelzle, M., G. Weissmueller, and E. Sackmann. 1993. On the application of supported bilayers as receptive layers for biosensors with electrical detection. *J. Phys. Chem.* 97:2974–2981.

Tamm, L. K., and H. M. McConnell. 1985. Supported phospholipid bilayers. *Biophys. J.* 47:105–113.

Tampé, R., and H.-J. Galla. 1991. Synargistic effects of Ca^{2+} and wheat germ agglutinin on the lamellar-hexagonal (H_{II}) phase transition of glycophorin-containing egg-phosphatidylethanolamine membranes. *Eur. J. Biochem.* 199:187–193.

Tanaka, T., and D. J. Fillmore. 1979. Kinetics of swelling of gels. *J. Chem. Phys.* 70:1215–1218.

Wu, E.-S., K. Jacobson, and D. Papahadjopoulos. 1977. Lateral diffusion in phospholipid multibilayers measured by fluorescence recovery after photobleaching. *Biochemistry.* 16:3936–3942.